

Numerical and theoretical investigation of bolted sleeve connections with rectangular hollow sections

<http://dx.doi.org/10.1590/0370-44672022760041>

Matheus Miranda de Oliveira^{1,3}

<https://orcid.org/0000-0002-4098-6383>

Lucas Roquete^{2,4}

<https://orcid.org/0000-0002-7937-822X>

Lucas da Silva Tanus^{2,5}

<https://orcid.org/0000-0002-8060-1337>

Isabella Estevão Monteiro^{2,6}

<https://orcid.org/0000-0003-1981-9916>

Vinicius Alves^{1,7}

<https://orcid.org/0000-0002-8572-0722>

Arlene Maria Cunha Sarmanho^{1,8}

<https://orcid.org/0000-0001-6900-8551>

¹Universidade Federal de Ouro Preto – UFOP, Escola de Minas, Departamento de Engenharia Civil, Ouro Preto – Minas Gerais - Brasil.

²Universidade Federal de São João del-Rei – UFSJ, Departamento de Tecnologia em Engenharia Civil, DTECH, Ouro Branco – Minas Gerais - Brasil.

E-mails : ³matheusmoliveira4@gmail.com,

⁴lucasroquete@gmail.com, ⁵lucas.tanus@hotmail.com,

⁶isabellamonteiro@gmail.com,

⁷vnichio@hotmail.com, ⁸arlene.sarmanho@gmail.com

Abstract

This article presents a theoretical and numerical study of bolted sleeve connections with rectangular hollow sections (RHS) under axial tension and compression. The geometric form of a hollow section provides resistance for high axial loads, torsion and combines effects, spreading its utilization in truss systems. In this context, the sleeve connections proposed explore these characteristics of RHS and offer an attractive aesthetic appearance for the continuity of elements. The bolted sleeve connection with RHS is formed by two outer tubes connected by an inner tube and staggered bolts. Herein, a parametric study was developed for identification of the failure modes in the connection. Finite element models with different geometric parameters and number of bolts were created in commercial software. The width, depth and thickness of RHS tubes and diameter of bolts were varied. In the theoretical/numerical/parametric results, the yielding gross section failure, the fracture through the effective net area failure and the bearing failure were observed. These failure modes occurred in both outer and inner tubes. The load results were compared to determine the resistance capacity of sleeve connections. The theoretical formulations were evaluated for representation of the ultimate load of the failure modes.

Keywords: sleeve connections, rectangular hollow sections, numerical analysis.

1. Introduction

Steel tubular profiles are used on a large scale in some parts of the world, including Europe, Southeast Asia, Australia and North America. These profiles offer a good solution for structural elements with possibly wide spans. Tubular profiles are lightweight and more economical due to their high strength and low weight. These profiles are widely used in trussed structural systems because the axial loads are predominant in these types of structural systems (Wardenier *et al.*, 2010).

For logistical, technical and manufacturing reasons, the tubes are divided into structures with a length shorter than that required for certain structures. Thus, a mechanism is needed to connect the tubes to allow their continuity from the structure.

In this context, there is an increase in investigations and studies related to the design and behavior of connections in tubular profiles that facilitate the structure assembly processes (Araujo *et al.*, 2016; Luo *et al.*, 2016; Xie *et al.*, 2019; Xing *et al.*, 2020).

Currently, the normative standard ABNT NBR 16239 (2013) only presents the flanged connections design as an option for splices between tubular profiles. This connection has been assessed by several researchers (Couchaux *et al.*, 2018, 2019; Deng *et al.*, 2018; Liu *et al.*, 2019).

Thus, to create a new design and aesthetic option, and to facilitate assembly, the sleeve connection was developed. This connection is composed of outer tubes connected by an inner tube and bolts. Ini-

tially, the sleeve connection was studied for circular hollow sections (CHS) by Amparo (2014), Amparo *et al.* (2015), Roquete *et al.* (2017), Roquete (2018), Oliveira (2019), Oliveira *et al.* (2020), Roquete *et al.* (2021) and Roquete *et al.* (2022). Figure 1 shows an example of sleeve connection with CHS evaluated by Roquete (2018).

Recently, Roquete *et al.* (2021) presented an extensive numerical, theoretical and experimental study for sleeve connections with steel CHS and staggered bolts. Five failure modes were described and evaluated, the yielding gross cross-section failure (YGCS), the fracture through the effective net cross-section failure (FNCS), the bearing failure (BF), the bolt bending (BB) and bolt shear (SB).



Figure 1 - Sleeve connection with CHS (Roquete, 2018).

However, the evaluation of sleeve connections with RHS was not performed and is the object of this re-

search. The bolted sleeve connection with RHS is composed of two outer tubes with rectangular sections con-

ected by staggered bolts to an inner tube with a smaller height and width, Figure 2.

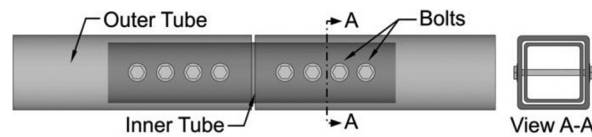


Figure 2 - Sleeve connection with RHS.

This article aims to study through theoretical and numerical analysis the behavior of 62 sleeve connections with aligned bolts and RHS under axial

tension and compression. A numerical parametric study was developed varying the height and the width of the inner and outer tubes and the number of bolts. The

results of FE models were compared with theoretical equations that determines the resistance capacity of the connection to verify the representability of equations.

2. Materials and methods

2.1 Numerical modelling

The numerical model by the Finite Element Method was established using the commercial software ANSYS 22R1 (2021). The finite element SHELL 181 was attributed to represent the RHS tubes. It is a homogeneous structural element with 4-node and six degrees of freedom at each node. The finite element SOLID 186 was adopted to represent the bolts. This element is defined by 20-node with three degrees of freedom per node.

The contact pair CONTA175 and TARGE170 was used to represent the contact between the bolts and the transverse

section of the RHS tube in the holes. The same finite elements were used by Oliveira *et al.* (2020), Roquete *et al.* (2021) and Roquete *et al.* (2022) for analysis of bolted sleeve connections with CHS.

The free mesh was adopted for all elements of the connection. For the RHS tubes, the mesh size was equal to 6 millimeters and the bolts equal to 5 millimeters. The behavior of the material characteristics was represented using the model of multilinear elastic material (Multilinear Isotropic Hardening), as presented by Salmon and Johnson (1990).

The boundary conditions were es-

tablished: the nodes at one end of the outer tubes were constrained to displacement and rotation in all directions; At the other end a displacement of 12.5 millimeters was applied in axial direction to simulate the axial tension and compression. A displacement incremental control was applied. The Newton-Raphson iterative method was adopted for the solution.

The final configuration of the FE model was illustrated in Figure 3. The geometrical and material properties of the numerical models developed will be presented in the next item.

2.2 Parametric study

A parametric study is essential for the progress of research on steel connections. Despite the absence of experimental results to validate the FE numerical model, the finite element characteristics similar to those adopted by Roquete *et al.* (2021) were used. Thus, the present study is an important contribution for assessment of the behavior and failure modes of the sleeve connection with RHS.

In the study, 62 FE models were elaborated with a variation of the geometry and

the number of bolts, divided into 31 models under axial tension and 31 models under compression. The FE models with similar properties were evaluated under axial tension and compression. The geometric properties of the sleeve connection models are presented in Table 1. In all models, the inner tube thickness was equal to 5mm to reduce the number of parameters that influence the connection. The bolt diameter (d_b) equal to 15 mm and hole diameter defined by adding a 1.5 mm was adopted in all

models. The hole distance from the edge of the tube and the distance from hole to hole were defined by the normative standard ABNT NBR 8800 (2008).

The mechanical characteristics of the models were: for the tubes, the yield stress equal to 250 MPa and ultimate tensile strength of 360MPa; for the bolt the yield stress equal to 635 MPa and ultimate tensile strength of 825MPa. The nominal Young's modulus was equal 200 GPa and Poisson's ratio of 0.30.

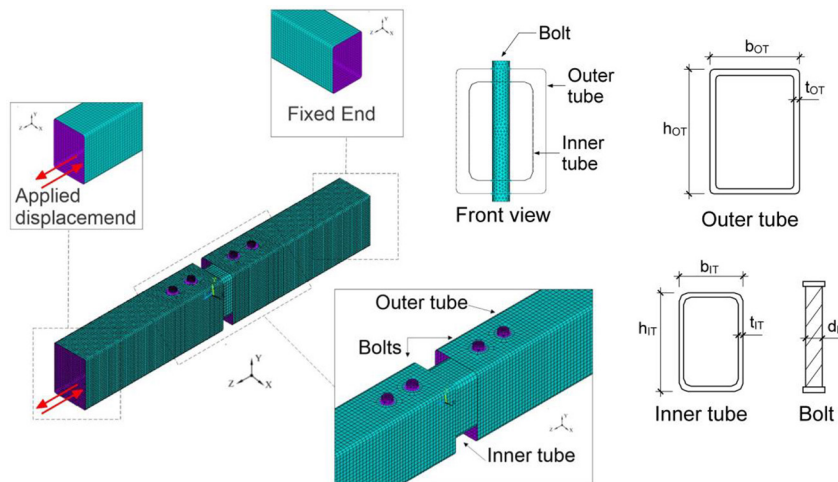


Figure 3 - FE numerical model.

Table 1 - Geometric data of the parametric study.

Model Number	Number of bolts	Outer tube			Inner tube*	
		Height [h _{OT}] (mm)	Width [b _{OT}] (mm)	Thickness [t _{OT}] (mm)	Height [h _{IT}] (mm)	Width [b _{IT}] (mm)
1	2	110	80	2.5	90	60
2	3					
3	4					
4	5					
5	2					
6	3					
7	4					
8	5					
9	2					
10	4					
11	5					
12	2					
13	3					
14	4					
15	5					
16	2					
17	3					
18	4					
19	5					
20	2	130	100	2.5	110	80
21	4					
22	5					
23	2					
24	3					
25	4					
26	5					
27	2					
28	3					
29	4					
30	5					
31	3	4.5				

*In all numerical models, the inner tube thickness (t_{IT}) was equal to 5 mm.

2.3 Failure Criterion

The fracture through the effective net cross-section failure (FNCS), bearing failure (BF) and yielding cross-section failure (YGCS) are the failure modes evaluated.

2.4 Theoretical review

Currently, the sleeve connection design is not included in normative standards. The failure modes verified in this article are based design formulation presented by Oliveira (2019) and Roquete *et al.* (2021).

Where: A_g – the cross-sectional area of RHS tubes; f_y – yield tensile stress of tubes;

The fracture through the effective net cross-section is described as the steel

The FNCS and BF were characterized when an excessive material deformation was observed. The failure was identified when the deformation of von Mises

In addition, the ultimate limit state of the tubes and bolts was evaluated according to ABNT NBR 8800 (2008).

The yielding gross cross-section failure is characterized the RHS

$$N_{c,Rk} = P_{teo} = A_g \times f_y \quad (1)$$

necking followed by the rupture of the element along the edge of the hole. The FNCS theoretical loading (P_{teo}) for sleeve connection with RHS was calculated according to Eq. (2) and (3), and

$$N_{t,Rk} = P_{teo} = A_e \times f_u \left\{ \begin{array}{l} A_e = C_t \times A_n \\ A_n = A_g - 2d_f t \\ C_t = 1 - \frac{e_c}{l_c}; e_c = \frac{d^2 + 2db}{4(d+b)} \end{array} \right\} \quad (2)$$

$$\text{for: } n > 4: l_c = l_{f1} + (n-1) l_{f2} \quad (3)$$

$$\text{for: } n > 4: l_c = l_{f1} + 3l_{f2}$$

Where: A_e – effective net area of tubes; A_n – net area of tubes; f_u – ultimate tensile strength; C_t – reduction factor due to holes presence; d_f – hole diameter; t – tube thickness; e_c – eccentricity of connection;

l_c – the effective length of the connection; l_{f1} – distance between the center of the hole and the edge of the tube distance between the center of the hole and the center of the adjacent holed; l_{f2} – distance between

reaches values higher than the ultimate rupture deformation. The YGCS occurred at moment of the peak load, when other failure modes have not been identified.

reaches the plastic deformation, exceeding the elastic deformation limit. The YGCS theoretical loading (P_{teo}) was calculated according to Eq. (1) and ABNT NBR 8800 (2008).

Roquete *et al.* (2021) and ABNT NBR 8800 (2008). The theoretical values representing the ultimate load resistance of bearing failure were given by Eq. (4), and ABNT NBR 8800 (2008).

the center of the hole and the center of the adjacent hole; d – width of the RHS tube; b – height of the RHS tube; and n – number of bolts connecting an outer tube to the inner tube.

$$N_{Rk} = P_{teo} = 2.4d_b \times t \times f_u \quad (4)$$

Where: t – tube thickness; d_b – bolt diameter; f_u – ultimate tensile strength;

3. Results

Table 2 presents the results obtained by the FE models and by the theoretical formulations. In addition, the failure modes and the location of occurrence are shown. Among the 31 FE models analyzed under compression, 23 failed by BF and 8 by YGCS. While for the 31 FE models evaluated under axial tension, 15 presented BF and 16 presented FNCS. The BF occurred in both outer tubes and inner tubes. The FNCS and YGCS was limited to the inner tubes.

Comparing the FE models and theoretical results (P_{num}/P_{teo}) for models under axial tension, the mean value of the P_{num}/P_{teo} ratio was equal to 0.87 and coef-

ficient of variation (CoV) of 0.241. For models evaluated under compression, the mean value of the P_{num}/P_{teo} ratio was equal to 0.83 and CoV of 0.218. Both mean value results indicate conservative numerical results compared to theoretical formulations.

Figure 4 shows the von Mises stress distribution in the models representing the three different failure modes identified. Figure 4a) represents the FNCS in the holes in the region central of the inner tube in the FE model M3. Figure 4b) illustrate the BF in the holes of the outer tube in the FE model M6 under axial tension. Finally, in Figure 4c), YGCS was observed in the central region of the inner tube of the FE

model M4 under compression.

However, it is necessary to prevent failure modes to occur in the inner tube of the connection, due to the impossibility of visual control, as recommended by Roquete *et al.* (2021). Thus, the models that presented failures in the inner tube were disregarded. The bearing failure was the only failure mode observed in the outer tubes. In this context, the mean value of the P_{num}/P_{teo} ratio increased to 0.97 with CoV of 0.22, for models under axial tension and compression, Figure 5. Therefore, Eq. 4 can satisfactorily represent the ultimate load of the bearing failure in the outer tubes.

Table 2 - Failure modes, numerical and theoretical results.

Model number	Connection under tension					Connection under compression					
	Failure mode	Tube failure	P _{num} (kN)	P _{teo} (kN)	P _{num} /P _{teo}	Failure mode	Tube failure	P _{num} (kN)	P _{teo} (kN)	P _{num} /P _{teo}	
1	BF	OUT	172.9	129.6	1.33	BF	OUT	148.08	129.6	1.14	
2	BF	OUT	255.33	194.4	1.31	BF	OUT	220.07	194.4	1.13	
3	FNCS	IN	331.56	414.88	0.8	BF	IN	318.21	518.4	0.61	
4	FNCS	IN	332.25	414.88	0.8	YGCS	IN	354.95	375	0.95	
5	BF	OUT	172.98	155.52	1.11	BF	OUT	158.23	155.52	1.02	
6	BF	OUT	255.44	233.28	1.09	BF	OUT	229.63	233.28	0.98	
7	FNCS	IN	331.34	414.88	0.8	BF	OUT	236.68	311.04	0.76	
8	FNCS	IN	332.27	414.88	0.8	YGCS	IN	353.39	375	0.94	
9	BF	OUT	170	181.44	0.94	BF	IN	171.61	259.2	0.66	
10	FNCS	IN	331.65	414.88	0.8	BF	OUT	285.44	362.88	0.79	
11	FNCS	IN	332.25	414.88	0.8	YGCS	IN	353.18	375	0.94	
12	BF	OUT	180.3	207.36	0.87	BF	OUT	168.7	207.36	0.81	
13	BF	OUT	269.09	311.04	0.87	BF	IN	246.19	388.8	0.63	
14	FNCS	IN	331.72	414.88	0.8	YGCS	IN	316.26	375	0.84	
15	FNCS	IN	332.25	414.88	0.8	YGCS	IN	294.12	375	0.78	
16	BF	OUT	179.74	233.28	0.77	BF	OUT	166.87	233.28	0.72	
17	BF	OUT	359.24	349.92	1.03	BF	OUT	228.49	349.92	0.65	
18	FNCS	IN	331.73	414.88	0.8	YGCS	IN	285.43	375	0.76	
19	FNCS	IN	332.26	414.88	0.8	YGCS	IN	290.94	375	0.78	
20	BF	OUT	168.26	129.6	1.3	BF	OUT	163.6	129.6	1.26	
21	BF	OUT	331.14	259.2	1.28	BF	OUT	307.13	259.2	1.18	
22	FNCS	IN	411.16	512.21	0.8	YGCS	IN	381.46	475	0.8	
23	BF	IN	170.93	259.2	0.66	BF	OUT	118.18	181.44	0.65	
24	FNCS	IN	255.08	473.46	0.54	BF	IN	247.97	388.8	0.64	
25	FNCS	IN	334.07	512.21	0.65	BF	OUT	299.78	362.88	0.83	
26	FNCS	IN	439.4	512.21	0.86	BF	IN	386.46	648	0.6	
27	BF	IN	162.73	259.2	0.63	BF	IN	165.77	259.2	0.64	
28	BF	IN	247.32	388.8	0.64	BF	IN	247.32	388.8	0.64	
29	FNCS	IN	338.54	512.21	0.66	BF	OUT	328.75	414.72	0.79	
30	FNCS	IN	411.53	512.21	0.8	BF	OUT	412.02	518.4	0.79	
31	BF	IN	337.79	388.8	0.87	BF	OUT	315.3	349.92	0.9	
Mean						0.87					
CoV						0.241					

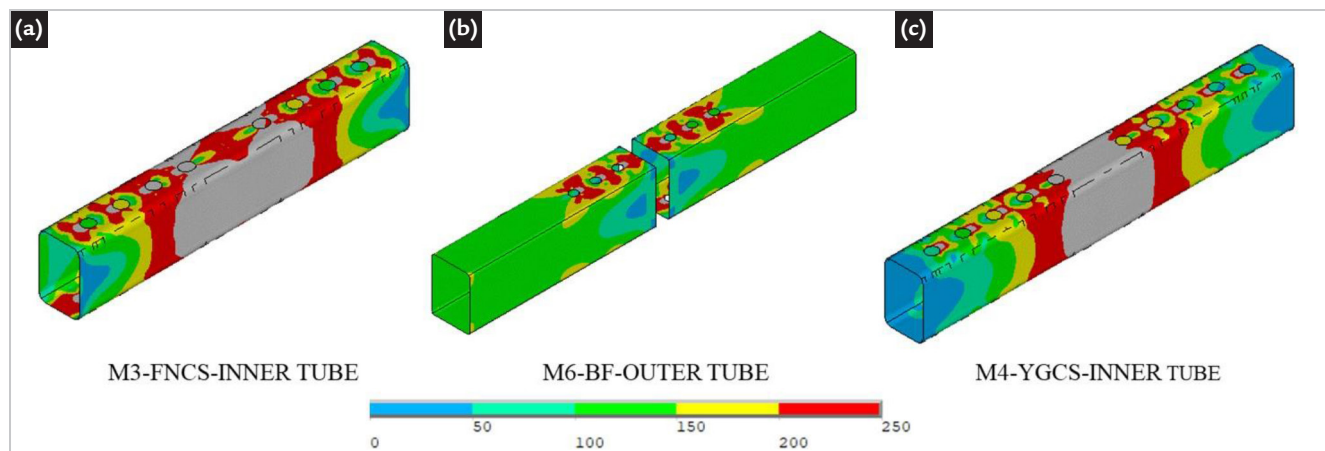


Figure 4 - Von Mises stress distribution of the FE models: a) M3-FNCS, b) M6-BF and c) M4-YGCS.

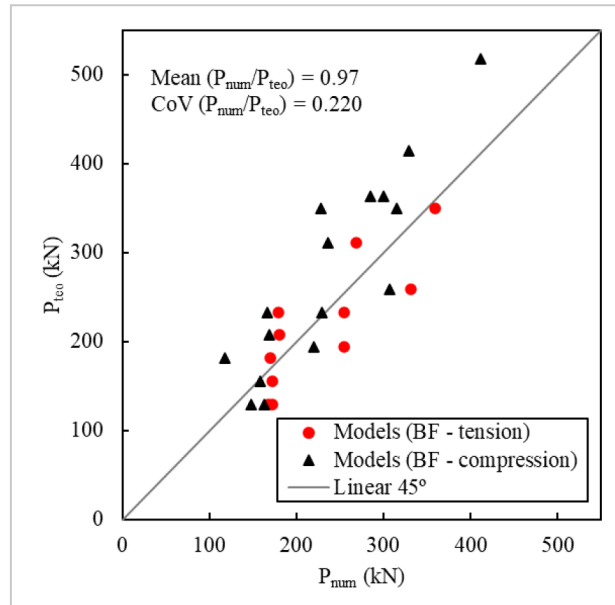


Figure 5 - Comparison between numerical and NBR 8800 ultimate loads.

Figure 6 shows the influence of the increase in the number of bolts on the resistance capacity of the sleeve connection through load-displacement curves. A high increase in the strength when the

number of bolts was increased from 2 to 3 bolts was observed. This increase was also identified when the number of bolts was from 3 to 4. However, no significant gain in resistance capacity was

observed when the sleeve connection was from 4 to 5 bolts. This behavior was also identified by Roquete *et al.* (2021) and Roquete *et al.* (2022) for sleeve connections with CHS.

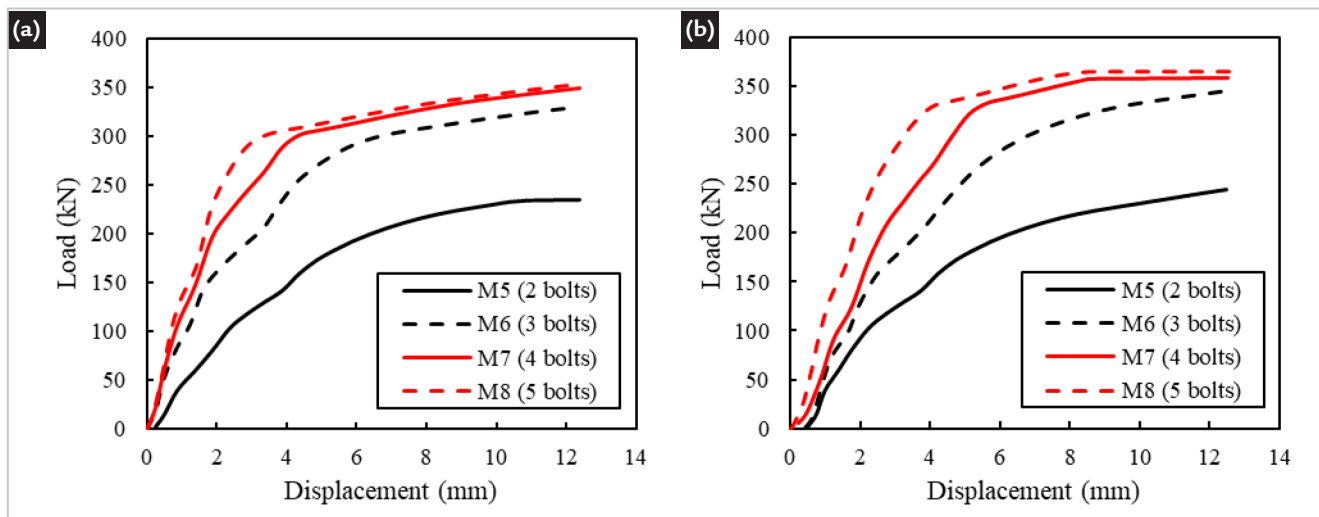


Figure 6 - Influence of number of bolts in the sleeve connection: a) under axial tension; b) under compression.

4. Conclusions

This article presented a theoretical and numerical study for the sleeve connection with RHS under axial tension and compression. A total of 62 models were evaluated: 31 models under axial tension and 31 under compression. The FE models allowed to verify the influence of the geometric parameters and number of bolts on the behavior of the connection. The fracture through the effective net cross-section failure (FNCS), bearing failure (BF) and yielding gross cross-section failure (YGCS) were the failure modes identified.

The numerical and theoretical

failure load of the sleeve connection were compared. The mean value of the P_{num}/P_{teo} was equal to 0.87 and CoV of 0.241 for connections under axial tension. And P_{num}/P_{teo} of 0.83 and CoV of 0.218 for connections under compression. The models with inner tube failure were discarded due to difficulty in visual control. The BF was the only failure mode that occurred in the outer tubes. Thus, the mean value of the P_{num}/P_{teo} increased to 0.97 and the theoretical formulation is adequate to represent the BF in outer tubes.

The influence of the number of bolts on the resistance capacity was presented using the load-displacement curves. The increase in the resistance capacity as the number of bolts increased was observed. However, for 4 and 5 bolts, the ultimate load was similar. It is suggested for future studies that an analysis be made of the optimal combination of number of loads per load gain in relation to the increase in the cost of the connection. In addition, experimental analyzes of the sleeve connection with RHS is recommended.

Acknowledgements

The authors are grateful for the support from FAPEMIG, CAPES, CNPq, UFSJ and UFOP.

References

- AMPARO, L. R. *Análise teórico-experimental de ligações tipo luva compostas por perfis tubulares com parafusos em linha e cruzados*. 2014, 80f. Dissertação (Mestrado em Engenharia Civil) - Escola de Minas, Universidade Federal de Ouro Preto, Ouro Preto, 2014.
- AMPARO, L. R.; SARMANHO, A. M.; ARAÚJO, A. H. M.; REQUENA, J. A. V. Analysis of the possible failure modes in CSH bolted sleeve connections. (E. Batista, Vellasco & Lima, Eds.) *In: INTERNATIONAL SYMPOSIUM TUBULAR STRUCTURES*, 15. *Anais [...]* Rio de Janeiro: 2015.
- ANSYS INC. *ANSYS Version 22R1*. EUA: Swanson Analysis System, 2021.
- ARAÚJO, A. H. M. de; SARMANHO, A. M.; BATISTA, E. de M.; REQUENA, J. A. V.; FAKURY, R. H.; PIMENTA, R. J. *Projeto de estruturas de edificações com perfis tubulares de aço*. Belo Horizonte: Ed. do Autor, 2016. 598 p.
- ASSOCIAÇÃO BRASILEIRA DE NORMAS TÉCNICAS. *NBR 8800*: projeto de estruturas de aço e de estruturas mistas de aço e concreto de edifícios. Rio de Janeiro: ABNT, 2008.
- _____. *NBR 16239*: projeto de estruturas de aço e de estruturas mistas de aço e concreto de edificações com perfis tubulares. Rio de Janeiro: ABNT, 2013.
- COUCHAUX, M.; HJIAJ, M.; RYAN, I.; BUREAU, A. Tensile resistances of bolted circular flange connections. *Engineering Structures*, v. 171, p. 817-841, sep. 2018.
- COUCHAUX, M.; HJIAJ, M.; RYAN, I.; BUREAU, A. Bolted circular flange connections under static bending moment and axial force. *Journal of Constructional Steel Research*, v. 157, p. 314-336, jun. 2019.
- DENG, H.; SONG, X.; CHEN, Z.; FU, P.; DONG, J. Experiment and design methodology of a double-layered flange connection in axial loads. *Engineering Structures*, v. 175, p. 436-456, nov. 2018.
- LIU, X.-C.; CUI, F.-Y.; JIANG, Z.-Q.; WANG, X.-Q.; XU, L.; SHANG, Z.-X.; CUI, X.-X. Tension–bend–shear capacity of bolted-flange connection for square steel tube column. *Engineering Structures*, v. 201, p. 109798, dec. 2019.
- LUO, F. J.; BAI, Y.; YANG, X.; LU, Y. Bolted sleeve joints for connecting pultruded FRP tubular components. *Journal of Composites for Construction*, v. 20, n. 1, p. 04015024, feb. 2016.
- OLIVEIRA, M. M. de. *Análise de ligações tipo luva sob compressão*. 2019, 93 f. Dissertação (Mestrado em Engenharia Civil) - Escola de Minas, Universidade Federal de Ouro Preto, Ouro Preto, 2019.
- OLIVEIRA, M. M. de; ROQUETE, L.; SARMANHO, A. M. C.; PEREIRA, D. J. R.; ALVES, V. Bearing failure in bolted sleeve connections with circular hollow sections under compression. *REM - International Engineering Journal*, v. 73, n. 2, p. 153-161, jun. 2020.
- ROQUETE, L. *Estudo de ligações tipo luva em perfis tubulares*. 2018, 220 f. Tese (Doutorado em Engenharia Civil) - Escola de Minas, Universidade Federal de Ouro Preto, Ouro Preto, 2018.
- ROQUETE, L.; OLIVEIRA, M. M. de; SARMANHO, A. M. C.; XAVIER, E. M.; ALVES, V. N. Behavior and design formulation of steel CHS with sleeve connections. *Journal of Constructional Steel Research*, v. 177, p. 106465, feb. 2021.
- ROQUETE, L.; OLIVEIRA, M. M. de; SARMANHO, A. M. C.; XAVIER, E. M.; NICCHIO, A. S. V. Design of sleeve connections with cross-bolted on circular hollow sections under axial tension. *Engineering Structures*, v. 250, p. 113393, jan. 2022.
- ROQUETE, L.; SARMANHO, A. M. C.; MAZON, A. A. O.; REQUENA, J. A. V. Influence of shear lag coefficient on circular hollow sections with bolted sleeve connections. *REM - International Engineering Journal*, v. 70, n. 4, p. 393-398, dec. 2017.
- SALMON, C. G.; JOHNSON, J. E. *Steel structures - design and behavior: emphasizing load and resistance factor design*. 3. ed., 1990.
- WARDENIER, J.; PACKER, J. A.; ZHAO, X.-L.; VEGTE, A. VAN DE. *Hollow sections in structural applications*. 2. ed. Genebra: CIDECT, 2010.
- XIE, L.; BAI, Y.; QI, Y.; WANG, H. Pultruded GFRP square hollow columns with bolted sleeve joints under eccentric compression. *Composites Part B: Engineering*, v. 162, p. 274-282, apr. 2019.
- XING, L.; CAO, Q.; ZHANG, R. Structural behaviour of inner set bolted joints in steel tubes under tension. *Advances in Structural Engineering*, v. 23, n. 8, p. 1601-1613, 13 jun. 2020.

Received: 3 July 2022 - Accepted: 10 October 2022.



All content of the journal, except where identified, is licensed under a Creative Commons attribution-type BY.